**Determining sulfur speciation in oxidatively crosslinked degradable polymers using sulfur K-edge X-ray absorption spectroscopy**

*Melissa A. Smith, U. L. D. Inush Kalana, George E. Sterbinsky, Tianpin Wu, Matthew K. Kiesewetter,* and Dugan Hayes**

Dr. Melissa A. Smith, Dr. U. L. D. Inush Kalana, Prof. Matthew K. Kiesewetter, and Prof. Dugan Hayes
Department of Chemistry, University of Rhode Island, Kingston, RI 02881, USA
E-mail: dugan@uri.edu, mkiesewetter@uri.edu

Dr. George E. Sterbinsky and Dr. Tianpin Wu
Advanced Photon Source, Argonne National Laboratory, Argonne, IL 60439, USA

Keywords: degradable polymers, organosulfur polymers, gold recovery, X-ray absorption spectroscopy

A new family of water-degradable elastic polymers prepared by oxidative crosslinking of the parent polythionolactones shows promise in a broad range of applications, but the compositions of these materials elude conventional analytical methods. Here we use sulfur K-edge X-ray absorption spectroscopy to quantify the amounts of thioether, disulfide, sulfone, sulfate ester, and thionester in each polymer and to rule out the presence of several other functional groups, including sulfonate, thiosulfonate, sulfate, and sulfoxide. We rationalize this speciation as a function of linker flexibility in the context of sulfinyl cycloaddition reactions and propose a mechanism of aggregation for the oxidized polymers. Our results correlate with swelling ratios but not with porosity nor crosslink density measurements, demonstrating the importance of pairing mechanical and chemical techniques when characterizing heterogeneous organic polymers. Finally, we take advantage of the proximity of the gold $M_{4,5}$-edges to the sulfur K-edge to analyze the binding and reactivity of Au(III) with the crosslinked polymers.

## 1. Introduction

The rich and diverse chemistry of lactone ring-opening polymerization (ROP) continues to play a dominant role in precisely tailored materials and niche applications, yet the chemistry of the corresponding heavy chalcogen congeners (sulfur-containing lactones, or

S-lactones) remains underexplored.[1,2] Polythionolactones in particular are largely unknown, not because they are intrinsically less useful than polyesters, but because they have been difficult to make by traditional methods.[1] In fact, the synthesis of polythionocaprolactone (PtnCL) by the Kiesewetter group in 2016 – accomplished via organocatalytic ROP of ε-thionocaprolactone – marked the first time a thionolactone was successfully opened to the corresponding polymer.[3] But because this remains one of only a small number of examples of such polymerizations, our understanding of the physical properties of poly(S-lactone)s and our access to copolymers and other advanced architectures remain limited.

The ability of sulfur to access high oxidation states adds new dimensions to the synthetic parameter space of the nascent family of thionolactone (co)polymers through both local oxidation and oxidative crosslinking reactions of thionocarbonyls. For example, the Kiesewetter group recently showed that treatment of polythionocaprolactone (PtnCL) with excess NaOCl results in the formation of an insoluble solid polymer with new material properties.[2] While PtnCL is an oil at room temperature, the Young's modulus of the oxidized product is consistent with those of elastic polymers. In addition, the material degrades in water, suggesting a multitude of potential applications: a degradable scaffold for drug delivery;[4] a solid surface to functionalize with amines, thiols and other nucleophiles;[5,6] a sacrificial functional group to protect natural rubbers from oxidation;[7] a synthon for the synthesis of dendritic or star shaped polymers;[8,9] and many others. The urgent need for degradable polymers with a broad spectrum of physical properties to curtail the accumulation of plastic waste makes this a particularly timely discovery. But to leverage the greatest advantage from this promising class of materials, the oxidation and/or crosslinking reaction(s) must be carefully and quantitatively characterized – a challenging objective for such presumably heterogeneous materials.

Several analytical techniques have been previously used to characterize the "spectroscopically silent" sulfur in organic polymers, but each has its own limitations.[10] For

example, $^{1}H$ and $^{13}C$ nuclear magnetic resonance spectroscopies must be performed in the solid state for insoluble polymers,[11–13] and thermogravimetric analysis is inherently destructive.[14] Common benchtop tools such as Fourier-transform infrared spectroscopy (FTIR),[15] Raman spectroscopy,[16,17] and X-ray photoelectron spectroscopy (XPS)[2,18] can be challenging because of spectral congestion between the characteristic frequency ranges of different sulfur-containing functional groups,[10] and powder X-ray diffraction[12,13] cannot provide meaningful information on the chemical environment of sulfur for amorphous materials.

Accordingly, we chose instead to measure the sulfur K-edge X-ray absorption near edge structure (XANES) spectra of the new family of crosslinked poly(S-lactone)s and related copolymers to identify the oxidized sulfur-containing functional groups and crosslinks. This non-destructive and element-specific method has been extensively[19] used to identify sulfur-containing compounds in complex matrices in the petroleum (e.g., kerogen, coal, asphalts),[20–31] biological (e.g., cells, tissues, biominerals),[32–42] archaeological,[43,44] agricultural,[45,46] and environmental and geological sciences (e.g., minerals, soils, aerosols, marine sediments).[47–54] In the context of sulfur-containing organic polymers, conventional XANES has been used to monitor polymer degradation upon exposure to heat,[55] electrical bias,[56,57] and ionizing radiation,[58] while angle-dependent XANES[59,60] and anomalous X-ray scattering at the sulfur K-edge[61–65] have been used to study the bulk and nanoscale morphology of semiconducting polymer films.

Importantly, sulfur K-edge X-ray absorption spectroscopy (XAS) is not simply a fingerprinting technique; instead, the sensitivity of the edge energy to oxidation state, chemical environment, and molecular structure often results in well-resolved absorption features that enable quantification of sulfur speciation in heterogeneous environments.[66–69] Additionally, the sulfur pre-edge provides a measure of metal-ligand covalency in proteins bearing sulfur-coordinated metallocofactors and corresponding model complexes.[70–74] And

despite the challenges inherent to working in the "tender" X-ray spectral region, where even ambient air strongly attenuates the beam, X-ray transient absorption at the sulfur K-edge has even been used to follow photochemical reactions of small molecules in real time.[75,76]

Here we show that we can determine the sulfur speciation in oxidatively crosslinked poly(S-lactone)s by fitting the sulfur K-edge XANES spectra to linear combinations of the spectra of small molecule reference compounds and a representative precursor polymer. Similar methods have been used previously to qualitatively characterize sulfur crosslinks in vulcanized rubbers,[77–79] but here, the chemical homogeneity of the uncrosslinked synthetic polymers permits a robust quantitative analysis. While our previous FTIR measurements of these materials confirmed that the uncrosslinked polymer linkages are thionoesters (**Scheme 1**), both FTIR and XPS proved inconclusive for identifying the crosslinks and/or oxidized group(s) in the crosslinked samples. The spectra are consistent, however, with mixtures of thioethers, thiols, disulfides, and/or sulfones,[2] and most of these possible moieties exhibit distinct, well-resolved sulfur K-edge spectra in organic and inorganic materials: disulfides may be easily distinguished from thioethers by the presence of a unique, well resolved 1s → σ* (S-S) peak below the common 1s → σ* (S-C) peak;[80,68,81,82] the K-edge of sulfoxides is approximately 2-3 eV higher than that of thioethers, thiols or disulfides;[26,83] and sulfones have a single, broad peak approximately 4 eV higher still.[84]

## 2. Methods

Three homopolythionolactones (polythionocaprolactone, PtnCL; polythionoheptalactone, PtnHL; and polythionopentadecalactone, PtnPDL) and a representative block copolymer (polythionopentadecalactone-*block*-caprolactone, PtnPDL-*b*-PtnCL) were synthesized and oxidatively crosslinked as described previously (**Scheme 1**).[2] For the sake of simplicity, the crosslinked polymers (CLPs) are denoted as PtnCL-CLP, PtnHL-CLP, PtnPDL-CLP, and PtnPDL-*b*-PtnCL-CLP, respectively. Although the extent of

crosslinking can be controlled to a degree by varying oxidation reaction time and conditions,[85] we chose to maximize the fraction of oxidized sulfur to facilitate the subsequent XANES measurements. The resulting solid, spongy CLP discs were mounted on a 3D printed stand. A sample of pristine PtnPDL was also measured to provide a spectrum of the unmodified thionoester starting material.

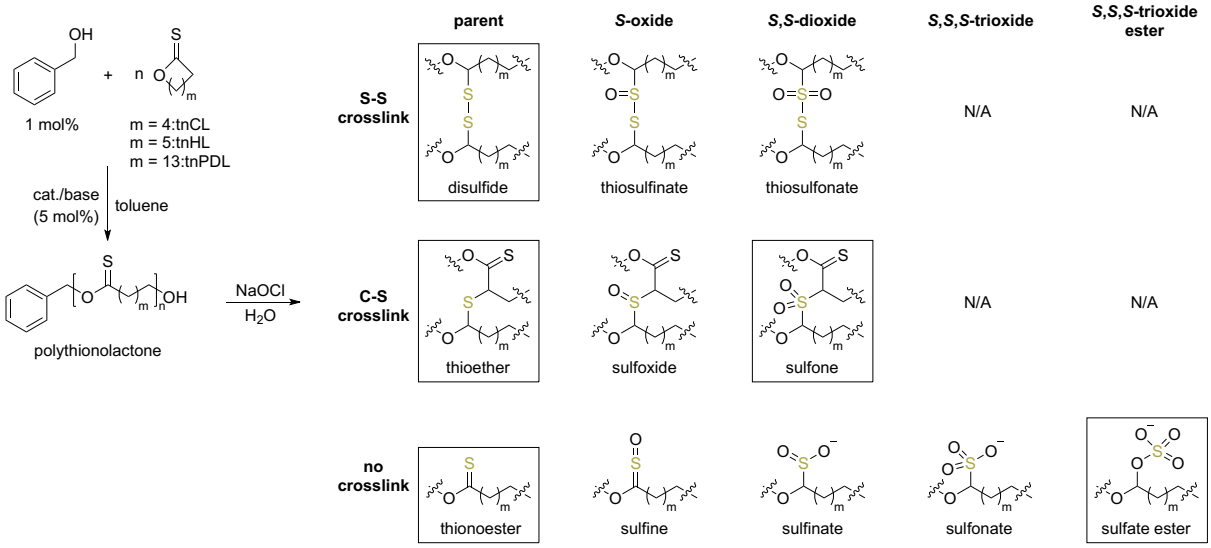


**Figure 1.** (Left) Organocatalytic ring-opening polymerization of thionolactones and subsequent oxidative crosslinking of polythionolactones. (Right) Structures of species potentially present in CLPs organized according to nature of crosslink (rows) and oxidation state of sulfur (columns). The sulfur atom(s) of the labeled functional groups are shown in mustard, and the species identified by sulfur K-edge XAS (*vide infra*) are outlined with boxes.

All sulfur K-edge and gold $M_{4,5}$-edge XANES spectra were measured at beamline 9-BM at the Advanced Photon Source at Argonne National Laboratory (Argonne, IL). Samples were measured at room temperature in a helium environment using the defocused beam (3x1 mm) to minimize sample damage during measurement. The energy axes of all spectra were calibrated by shifting the global maximum of the sodium thiosulfate reference spectrum to 2479.95 eV, in accordance with Ochmann *et al.*[76] (see SI for details). All spectra were acquired using fluorescence detection, a method that is known to be highly sensitive to sulfur concentration.[20,68,84] The CLPs range in composition from 12% (PtnPDL-CLP) to 24% (PtnCL-CLP) sulfur by mass, but the highly porous, spongy nature of these materials likely

mitigates much of the self-absorption that would be expected for dense solids with comparable compositions; indeed, the maxima ("white lines") at 2471.8 eV only differ in magnitude by 4% for all CLP spectra measured. To avoid thickness-induced attenuation and distortion of the XANES features in the spectra of solid reference compounds, those samples were diluted to a sulfur concentration of ~2% by mass using polyethylene glycol and thoroughly homogenized.

Linear combination analysis (LCA) was used to quantify sulfur speciation from the XANES spectra in accordance with Pickering *et al*.[68] We assembled a library of 24 spectra of 14 distinct organosulfur functional groups, which includes the spectra of the four reference compounds measured in this work and 20 spectra taken from the literature.[20,40,68,76,82,84,86,87] To ensure that thickness effects would not impact the LCA fits, we relied upon spectra of dilute solutions of model compounds measured by fluorescence or spectra of neat powders measured by total electron yield whenever possible. The energy axes of all literature spectra were also shifted to a common calibration following Ochmann *et al*.[76] The substances, sample conditions, energy axis shifts, and references for all 24 spectra used in LCA fitting are collected in **Table S1**.

LCA fits were performed using MATLAB (R2019b) using the amplitude and energy axis shift of each fit component as fit parameters. The energy axis of each LCA component was allowed to vary by ±1.0 eV and interpolated to that of the CLP spectrum using a cubic spline; in all cases, the fits converged to solutions with shifts less than 1 eV in magnitude. All four CLP spectra were fit between 2465 and 2485 eV to linear combinations of the PtnPDL thionoester reference spectrum and all possible combinations of 1, 2, 3, 4, and 5 other reference spectra (over 4.2M combinations). The spectra of both PtnPDL-CLP and PtnPDL-*b*-PtnCL-CLP were fit best to combinations of thionoester, disulfide, thioether, sulfone, and sulfate ester spectra; addition of a sixth component improved the fit but only by including an additional disulfide component. The spectra of PtnCL-CLP and PtnHL-CLP were fit best to

combinations of the same thionoester, disulfide, and sulfate ester spectra with minor contributions from additional disulfide and thiol components. Accordingly, we chose to fit all four CLP spectra to the same five reference spectra (highlighted in **Table S1**), though we cannot conclusively rule out the presence of thiols (*vide infra*).

## 3. Results and Discussion

### 3.1. Sulfur K-edge XANES

The enormous breadth of accessible oxidation states in organosulfur chemistry results in sulfur K-edge XANES spectra with white line energies ranging from 2469 eV for thioketones[32] to 2482 eV for sulfate esters.[33] This nearly continuous variation in peak energy as a function of sulfur oxidation has been previously presented by George and coworkers,[20,68] among many other groups. To organize our discussion here, we break down this range of possible peak energies into low (2469-2473 eV), intermediate (2473-2478 eV) and high (2478-2482) energies. Conveniently, these also correspond respectively to typical peak energies for species with low- (thioketones, disulfides, thiols, thioethers, elemental sulfur), intermediate- (sulfoxides, sulfinates, sulfines, inorganic sulfite), and high-valent sulfur (sulfones, sulfonates, sulfate esters, inorganic sulfate); the spectra of functional groups with sulfur in multiple oxidation states (e.g., thiosulfinates and thiosulfonates) generally exhibit multiple well-resolved peaks. We note that for the sake of simplicity, our discussion excludes the rich chemistry of heteroaromatic, sulfur-nitrogen, and sulfur-halide organic compounds, as we have no reason to expect these moieties to be present in our polymer samples.

The normalized spectrum of PtnPDL presented in **Figure 1B** is in excellent agreement with that of previously published thioketones,[32,88–90] showing a low-energy white line at 2469.8 eV corresponding to the 1s → (C=S)π* transition followed by a 1s → (C-S)σ* peak at 2473.2 eV. The CLP spectra in **Figure 1C-F** (shown alongside their LCA fits and individual

fit components scaled by their respective LCA weights) are dramatically different from that of PtnPDL, showing a clear ~2 eV shift of the white line to the far end of the low energy region at ~2472 eV as well as a new feature in the high energy region that reaches a maximum at ~2482 eV and exhibits several shoulders that extend into the intermediate energy region. Notably, the four CLP materials may readily be grouped into two pairs of nearly indistinguishable spectra – PtnCL-CLP and PtnHL-CLP in one and PtnPDL-CLP and PtnPDL-*b*-PtnCL-CLP in the other – with the major distinction between the pairs being the magnitude of the high-energy feature.

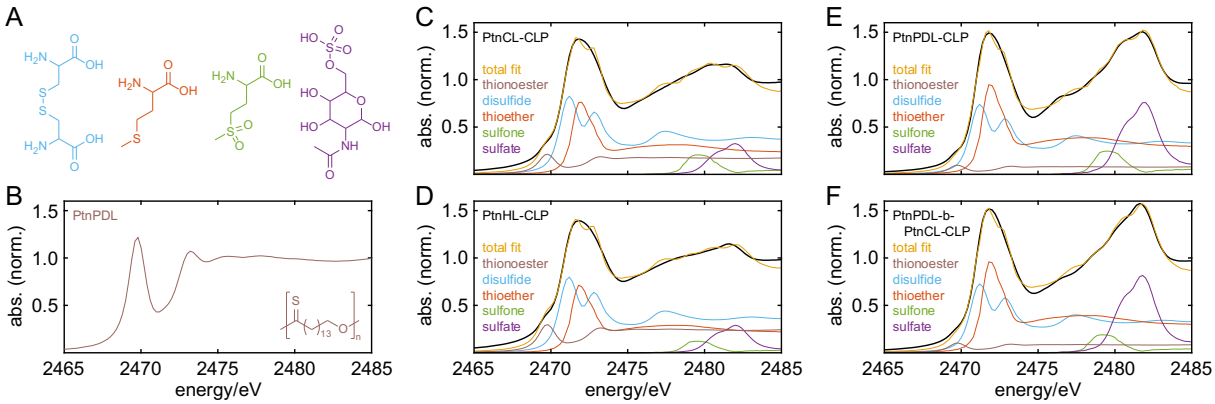


**Figure 1.** LCA of CLP sulfur K-edge XANES spectra. (A) Structures of (left to right) disulfide, thioether, sulfone, and sulfate ester reference compounds. (B) Normalized XANES spectrum and structure of uncrosslinked PtnPDL, which was used as the starting material (thionoester) reference. (C) – (F) Spectrum (black) and LCA fit (orange) of PtnCL-CLP (C), PtnHL-CLP (D), PtnPDL-CLP (E), and PtnPDL-*b*-PtnCL-CLP (F) plotted with weighted fit components (brown, blue, red, green, and purple).

### 3.2. Linear combination analysis

All CLP spectra show a small low energy shoulder at ~2468.5 eV that is captured in the LCA fits by the white line of the thionoester spectrum, indicating that this shoulder most likely corresponds to unreacted starting material. The peak centered at ~2472 eV also clearly corresponds to low-valent sulfur species, but its unusually broad linewidth (>3 eV fwhm) suggests significant chemical heterogeneity as expected for these materials. The best LCA fits of this feature for all CLP spectra correspond to sums of the disulfide and thioether standard spectra, though we cannot conclusively rule out contributions to this peak from thiols as well.

The individual fit components show that the peak is well reproduced by this combination because the thioether peak falls between the two characteristic disulfide peaks, giving a single, broad feature.

The lack of strong absorption and/or well-resolved peaks across the intermediate energy region is immediately apparent. Sulfines should exhibit two strong peaks at 2472.5 and 2475.2 eV,[36] while sulfoxides or sulfinates should exhibit sharp white lines at 2475 or 2476.5 eV, respectively.[36,91] Although the weak shoulder at 2476 eV that is particularly apparent in the PtnPDL-CLP spectrum initially appears to be consistent with sulfinates, our LCA procedure never converged to fit with more than a 0.4% contribution from the corresponding standard spectrum. Accordingly, we conclude that any such species are either entirely absent or present in very low relative concentrations in our Ptn-CLP materials.

As with the low energy feature, the broad, asymmetric nature of the high energy feature reflects a high degree of chemical heterogeneity. The best LCA fits correspond to sums of the sulfone and sulfate ester standard spectra, but as was the case with thiols, we cannot conclusively rule out contributions from sulfonates. The characteristic sulfate ester white line and shoulder at 2482 and 2481 eV, respectively,[40] are clearly present in all CLP spectra, while the broad sulfone peak accounts for the absorption extending toward lower energies. We expected that inorganic sulfate would not be present due to the aqueous environment in which the crosslinking step takes place, and indeed, the CLP spectra do not show evidence of the strikingly intense sulfate white line, which is generally reported to have a peak amplitude >7 in normalized spectra.[40,68,82,84,86]

While we previously attributed the presence of a strong band at ~1180 $cm^{-1}$ in the FTIR spectrum of PtnPDL to a thionoester C=S stretch,[2] the comparable band that appears in the spectrum of PtnPDL-CLP could have potentially corresponded to thioketones (including thionoesters), sulfones, sulfonates, sulfate esters, or combinations thereof.[92] XPS analysis of PtnPDL-CLP at the C 1s and S 2p cores was also consistent with the presence of thioketones

and/or sulfones but suggested disulfides may be present as well.[93,94] The XANES spectra presented here confirm that the starting thionoester polymers do indeed largely convert to mixtures of disulfides, thioethers, sulfones, and sulfate esters.

The relative amounts of starting material and products in the CLP samples obtained from the LCA fits are given with corresponding 95% confidence intervals in **Table 1** and visualized in **Figure 2** to facilitate comparison. The complete set of fit parameters, including the relative energy shifts of each LCA component, is given in **Table S2**. While the spectra in **Figure 1** qualitatively demonstrate the similarity in sulfur speciation for the small lactone CLPs (PtnCL-CLP and PtnHL-CLP) and separately for the macrolactone (PtnPDL-CLP) and block (PtnPDL-*b*-PtnCL-CLP) CLPs, we now consider these comparisons quantitatively. The small lactone CLPs retain more than twice as much of the starting thionoester than the other two, while all CLPs contain approximately the same amount of disulfide and only marginal amounts (<5 %) of sulfone. The additional oxidized sulfur in the macrolactone/block materials corresponds to a substantially higher amount of thioether (39% for macrolactone/block vs. ~30% for small lactones) and sulfate ester (~12% vs. ~5%), with the latter giving rise to the notably stronger high energy feature.

**Table 1.** Percent composition of sulfur-containing functional groups in CLPs

| | thionoester | disulfide | thioether | sulfone | sulfate ester |
|---|---|---|---|---|---|
| PtnCL-CLP | 20 ± 3 | 39 ± 4 | 31 ± 3 | 3.7 ± 0.8 | 5.0 ± 0.6 |
| PtnHL-CLP | 28 ± 3 | 37 ± 3 | 28 ± 3 | 2.1 ± 0.7 | 4.3 ± 0.5 |
| PtnPDL-CLP | 9 ± 3 | 35 ± 3 | 39 ± 3 | 4.4 ± 0.7 | 11.7 ± 0.5 |
| PtnPDL-*b*-PtnCL-CLP | 10 ± 3 | 35 ± 4 | 39 ± 3 | 3.4 ± 0.7 | 12.5 ± 0.6 |

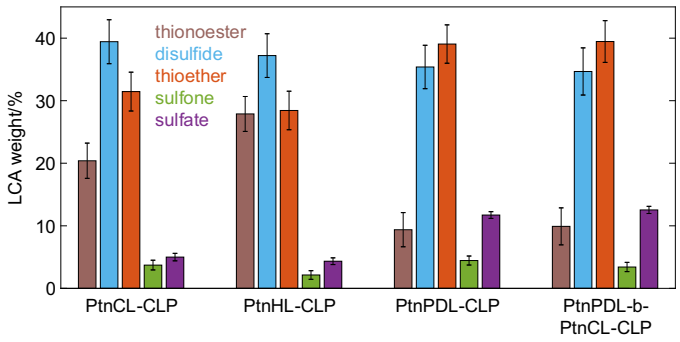


**Figure 2.** LCA weights of various sulfur-containing functional groups obtained from fits of the sulfur K-edge spectra of each CLP sample.

### 3.3. Chemical and physical insights

These trends in sulfur speciation are consistent with the hypothesis presented in our previous work[2] (which in turn followed the work of Block and coworkers[95]) that crosslinking C-S bonds (e.g., those yielding thioethers and sulfones) are formed upon exposure to bleach following the [4 + 2] cycloaddition of two sulfinyl intermediates generated by *S*-oxidation of the starting thionoesters. Such reactions would require alignment of the sulfinyl groups, a condition less likely to be met in polymers with only very short alkyl chains linking the thionoester monomers when compared to those with all (PtnPDL-CLP) or even some (PtnPDL-*b*-PtnCL-CLP) long alkyl chains. We also expect the non-crosslinking sulfate ester groups to arise from similar cycloaddition (and possibly subsequent cycloelimination) chemistry. Crosslinking disulfide bonds, on the other hand, can be formed irrespective of C=S/C=S bond dihedral angle and thus appear in roughly the same proportion in all CLP samples. And because of the interchain conformational dynamics within the fluid polymer phase in aqueous suspension during oxidation (PtnXL have lower melting points than their polylactone analogues[2]), nearly the same speciation is observed when all (PtnPDL-CLP) or only half (PtnPDL-*b*-PtnCL-CLP) of the alkyl chains are sufficiently long.

Because such cycloaddition chemistry first requires the generation of sulfines, however, this explanation may initially seem at odds with the absence of any sulfine XAS signal in the intermediate energy region. However, aliphatic thionoester sulfines are known to

be unstable at room temperature, decomposing within hours via to the corresponding esters with concomitant loss of sulfur.[96] This explanation is further supported by the appearance of a strong C=O stretching peak at 1728 $cm^{-1}$ in the FTIR spectrum of PtnPDL-CLP that is almost entirely absent in the uncrosslinked PtnPDL sample,[2] consistent with the conversion of some thionoesters to non-crosslinking esters during the oxidation process.

When comparing these results to those presented in our previous work, we find that the same pairs of CLPs also show similarly good agreement in swelling ratio, defined as the ratio of the mass of solvent absorbed by a sample of CLP to the mass of the sample (4.6 ± 0.01 and 5.16 ± 0.02 for PtnCL-CLP and PtnHL-CLP, respectively; and 9.40 ± 0.03 and 9.72 ± 0.25 for PtnPDL-CLP and PtnPCL-*b*-PtnCL-CLP, respectively). However, the porosities differed substantially for all four CLPs, showing a systematic increase in going from PtnCL-CLP to PtnHL-CLP to PtnPDL-CLP and finally to PtnPDL-*b*-PtnCL-CLP; similarly, the same series showed a systematic *decrease* in crosslink density (see Table S3). We believe these trends are consistent with a model of polymer aggregation illustrated in **Figure 3** in which the sulfones and sulfate esters promote formation of microscopic micellar domains to maximize solvation of these polar groups at the surface and minimize solvent exposure of the otherwise nonpolar polymer chains. The greater proportion of polar groups relative to total sulfur but lower overall sulfur content in PtnPDL-CLP and PtnPDL-*b*-PtnCL-CLP facilitates the formation of such domains and their subsequent fusion into even larger domains, giving rise to the meso- and macroscopic pores observed in those materials.[2] And because this process would also continuously refresh the solvent-exposed surface of the suspended polymer, a greater proportion of the starting thionoester is ultimately oxidized rather than being trapped in the bulk. The micellar structure also explains why the disulfide/thioether peak is larger than the sulfone/sulfate ester peak in the bulk-sensitive XANES measurements presented here but the opposite trend is seen in the surface-sensitive sulfur 2p XPS measurements presented in our previous report.[2] Crucially, the XANES data presented here reveal that while swelling

ratio could be a reliable lab-based metric for qualitative analysis of sulfur speciation in these materials, porosity and crosslink density are not directly correlated with the chemical structure following oxidation.

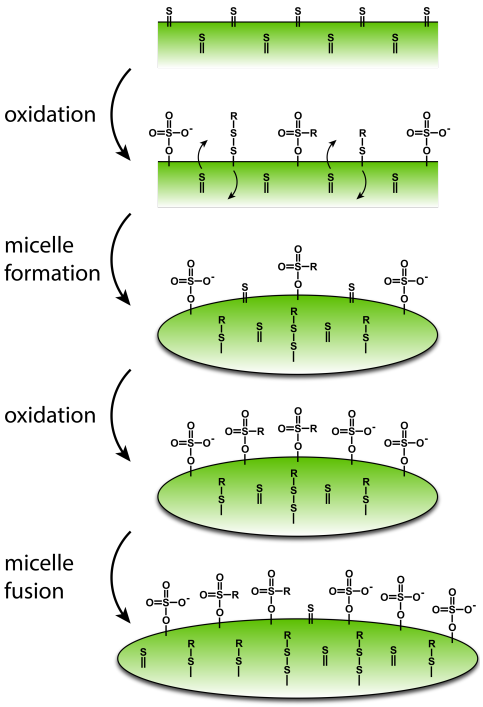


**Figure 3.** Sequential model of oxidative crosslinking and aggregation for PtnPDL-CLP and PtnPDL-*b*-PtnCL-CLP. The surface-exposed thionoesters are oxidized to a mixture of thioethers, disulfides, sulfones, and sulfate esters, which then promotes formation of micelles that keep the polar groups at the surface while burying the nonpolar groups in the bulk. Thionoesters migrate from the bulk to the surface during this process and are then oxidized as well. Finally, these micelles fuse and aggregate to give a mesoporous/microporous material.

### 3.4. Gold binding analysis

The strong affinity between sulfur and gold makes sulfur-rich materials excellent candidates for recovery of gold from electronic and industrial manufacturing waste streams.[97–101] We previously demonstrated that these insoluble CLPs can effectively sequester Au(III) from aqueous solution,[2] but we did not attempt to determine the nature and extent of the S-Au bonding. Fortunately, the gold $M_{4,5}$-edges are within 300 eV of the sulfur K-edge, making it convenient to probe both elements during the same experiment at a tender X-ray beamline. Despite the practical challenges associated with this energy regime, $M_{4,5}$-edge XAS is frequently used to quantify oxidation state in lanthanide-containing materials

due to their well-resolved, dipole-allowed 3d → 4f transitions.[102,103] Similar applications are far less common for gold[104] and other metals with fully occupied 4f orbitals where $L_{2,3}$-edge XAS is more straightforward and informative,[105–109] but the proximity of the sulfur and gold edges makes such multi-element measurements enticing.

The normalized sulfur K-edge spectra of PtnPDL-CLP before and after exposure to a dilute solution of tetrachloroaurate (see Methods for details) are shown in **Figure 4A**. While the low energy feature is essentially unchanged, the high energy feature appears to be substantially attenuated, more closely resembling that of the small lactone CLPs than that of the parent PtnPDL-CLP. However, integration of the spectra between the local minima at 2474.8 and 2484.2 eV (indicated by the vertical lines) reveals that the total absorption actually decreases by less than 2% upon exposure to Au(III); the feature only appears attenuated because it broadens toward lower energies. In comparison, integration of the same region in the small lactone CLP spectra shows a decrease of 7.5%.

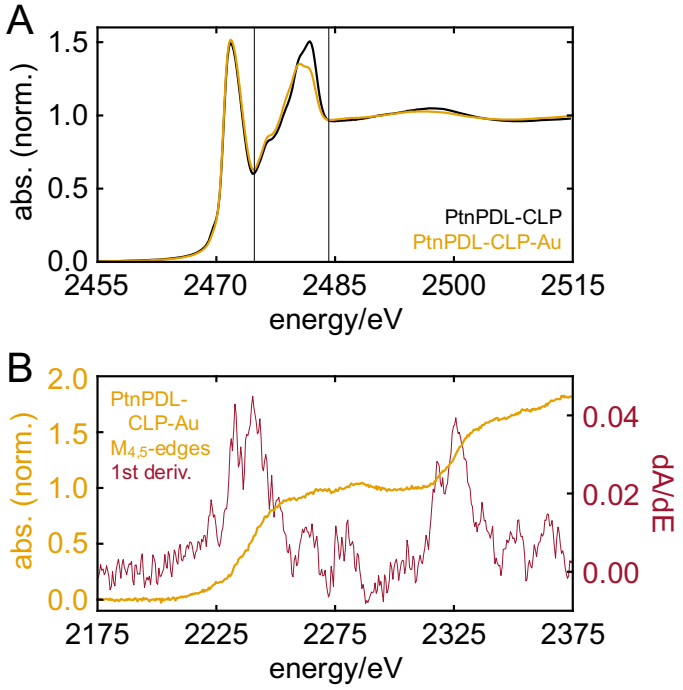


**Figure 4.** Multi-element XAS analysis of PtnPDL-CLP-Au. (A) Normalized sulfur K-edge spectra of PtnPDL-CLP before (black) and after (orange) exposure to aqueous Au(III). The vertical lines indicate the spectral region over which the integration discussed in the main text was performed. (B) Normalized gold $M_{4,5}$-edge spectrum (orange) and corresponding first derivative (crimson) of PtnPDL-CLP-Au.

This result suggests that the sulfone and/or sulfate ester groups, despite lacking lone pairs on the sulfur atoms, are more strongly affected by Au(III) than the disulfides and thioethers. And though Au(III) is known to oxidize disulfides to sulfonic acids[110] and thioethers to sulfoxides,[111] the fact that the magnitude of the low energy feature relative to the normalized edge step is unchanged upon exposure of the CLP to Au(III) solution suggests that those groups are not substantially oxidized. While these observations may initially seem surprising, they are in fact consistent with the model proposed above in which the disulfide and thioether groups are largely buried within the hydrophobic interior of the bulk polymer and the sulfone and sulfate ester groups are localized at the surface and thus more likely to interact with aqueous Au(III) ions. Au(III) metallosulfones[112] and sulfonates[113] have indeed been recently reported and represent possible motifs for such interactions, while Au(I) produced from the oxidation of disulfide by Au(III) could also be readily coordinated by the solvent-exposed groups.[114] Additionally, the apparent broadening of the high energy feature(s) and increase in absorption intensity across the intermediate energy region is consistent not only with the formation of sulfonic acids and/or sulfoxides but also the presence of $1s \rightarrow (Au\text{-}S)\sigma^*/\pi^*$ transitions following gold chemisorption.[105,106,115] The expected proliferation of spectral features due to chemisorption and/or Au-S redox chemistry renders our LCA method unreliable for this spectrum; instead, we simply conclude that while some redox chemistry likely does occur, chemisorption by the surface-exposed, highly-oxidized sulfur groups is the primary mode of CLP-Au(III) interaction in aqueous solution.

The gold $M_{4,5}$-edge spectrum normalized to the $M_5$-edge step and the corresponding first derivative spectrum are presented in **Figure 4B**. We note that the maxima of the $M_5$ and $M_4$ first derivatives appear at 2240.3 and 2325.8 eV, approximately 35 eV higher than the corresponding binding energies typically found in reference tables.[116] However, this shift is not reflective of the oxidation state of the gold measured here but instead is known to arise from the exceptionally broad range of energies spanned by the $3d \rightarrow (n \geq 6)p$ and $3d \rightarrow (n \geq$

5)f transitions.[117] In fact, both the absorption and first derivative spectra are in excellent agreement with those published by Owens *et al.* for metallic gold.[117] Because the energy axis was calibrated at the sulfur K-edge rather than the gold $M_{4,5}$-edge, however, the absolute calibration in this energy range likely has an error of 1-2 eV, and thus we cannot draw conclusions regarding Au(III), Au(I), and Au(0) speciation in this material without additional spectra of reference compounds. Nevertheless, the excellent signal observed at the gold $M_{4,5}$-edge provides proof of principle for such analyses.

## 4. Conclusion

We have demonstrated that sulfur K-edge XANES can be an effective tool for quantifying sulfur speciation in complex macromolecular systems and used this approach to analyze a family of four oxidatively crosslinked, water-degradable polythionolactones. Following the same oxidative treatment, the macrolactone polymers show a greater extent of sulfur oxidation and higher proportions of thioether and sulfate ester functional groups when compared to the small lactone polymers, possibly due to a greater likelihood of favorable C=S bond alignment for cycloaddition. The two modes of sulfur speciation are consistent with a model of CLP aggregation from micellar domains that also explains the results of the gold-binding studies presented here and the XPS, FTIR, and porosity measurements published previously. While the apparent correlation between XANES spectrum and swelling ratio among the materials studied here suggests that a simple, non-spectroscopic method can provide qualitative insight into sulfur speciation, further work is necessary to confirm this correlation and explore its scope. Finally, we have demonstrated the viability of tandem sulfur K-edge/gold $M_{4,5}$-edge spectroscopic methods for characterizing the binding of gold ions by sulfur-containing polymers, which will guide efforts toward improving such materials for industrial recovery applications.

Although we only present *ex situ* XANES measurements here, this work lays the foundation for using sulfur K-edge XANES to probe the dynamics of organocatalytic ring-opening polymerization reactions[118,119] in real time. And because the polymerization of polythionolactones may be carried out under neat conditions,[120] there is no need to contend with the often prohibitively strong attenuation of tender X-rays by solvent. Quick-scanning XAS with sub-second temporal resolution[121–123] may thus prove an essential tool for optimizing conditions (catalyst structure, catalyst loading, temperature, etc.) for a broad range of such reactions

**Supporting Information**
Supporting Information is available from the Wiley Online Library or from the author.

**Acknowledgements**
This research was supported by an NSF CAREER Award (CHE 1554830). Acknowledgment is made to the Donors of the American Chemical Society Petroleum Research Fund for support of this research, which supported all work by M.A.S. and D.H. This research used resources of the Advanced Photon Source, a U.S. Department of Energy (DOE) Office of Science User Facility operated for the DOE Office of Science by Argonne National Laboratory under Contract No. DE-AC02-06CH11357. All XAS spectra were measured at beamline 9-BM at the Advanced Photon Source, Argonne National Laboratory.

Received: ((will be filled in by the editorial staff))
Revised: ((will be filled in by the editorial staff))
Published online: ((will be filled in by the editorial staff))

References

[1] H. R. Kricheldorf, G. Schwarz, *Journal of Macromolecular Science, Part A* **2007**, *44*, 625–649.
[2] U. L. D. I. Kalana, P. P. Datta, R. S. Hewawasam, E. T. Kiesewetter, M. K. Kiesewetter, *Polym. Chem.* **2021**, *12*, 1458–1464.
[3] P. P. Datta, M. K. Kiesewetter, *Macromolecules* **2016**, *49*, 774–780.
[4] M. Feng, B. Tang, S. H. Liang, X. Jiang, *Curr Top Med Chem* **2016**, *16*, 1200–1216.
[5] D. Zheng, Y. Li, Y. An, J. Wu, *Chem Commun (Camb)* **2014**, *50*, 8886–8888.
[6] R. Sato, T. Senzaki, Y. Shikazaki, T. Goto, M. Saito, *Chem. Lett.* **1984**, *13*, 1423–1426.
[7] A. Früh, H.-J. Egelhaaf, H. Hintz, D. Quinones, C. J. Brabec, H. Peisert, T. Chassé, *Journal of Materials Research* **2018**, *33*, 1891–1901.
[8] R. Dong, Y. Zhou, X. Zhu, *Acc. Chem. Res.* **2014**, *47*, 2006–2016.
[9] H. Li, J. Sun, H. Zhu, H. Wu, H. Zhang, Z. Gu, K. Luo, *WIREs Nanomedicine and Nanobiotechnology* **2021**, *13*, e1670.

[10] A. S. M. Ghumman, M. M. Nasef, M. R. Shamsuddin, A. Abbasi, *Polymers and Polymer Composites* **2021**, *29*, 1333–1352.
[11] A. Hoefling, D. T. Nguyen, Y. J. Lee, S.-W. Song, P. Theato, *Mater. Chem. Front.* **2017**, *1*, 1818–1822.
[12] D. J. Parker, H. A. Jones, S. Petcher, L. Cervini, J. M. Griffin, R. Akhtar, T. Hasell, *J. Mater. Chem. A* **2017**, *5*, 11682–11692.
[13] S. Oishi, K. Oi, J. Kuwabara, R. Omoda, Y. Aihara, T. Fukuda, T. Takahashi, J.-C. Choi, M. Watanabe, T. Kanbara, *ACS Appl. Polym. Mater.* **2019**, *1*, 1195–1202.
[14] A. Abbasi, M. M. Nasef, W. Z. N. Yahya, M. Moniruzzaman, A. S. M. Ghumman, *European Polymer Journal* **2021**, *143*, 110202.
[15] Y. Tang, C. Chen, X. Li, Q. Wei, X. Guo, R. B. Finkelman, W. Li, X. Huan, *Energy Exploration & Exploitation* **2021**, *39*, 336–353.
[16] D. Cho, J. R. Rouxel, S. Mukamel, G. Kin-Lic Chan, Z. Li, *Journal of Physical Chemistry Letters* **2019**, *10*, DOI 10.1021/acs.jpclett.9b02414.
[17] R. J. H. Clark, in *Studies in Inorganic Chemistry* (Eds.: A. Müller, B. Krebs), Elsevier, **1984**, pp. 221–234.
[18] E. Cato, A. Rossi, N. C. Scherrer, E. S. B. Ferreira, *Journal of Cultural Heritage* **2018**, *29*, 30–35.
[19] F. Jalilehvand, *Chem. Soc. Rev.* **2006**, *35*, 1256–1268.
[20] G. N. George, M. L. Gorbaty, *J. Am. Chem. Soc.* **1989**, *111*, 3182–3186.
[21] S. R. Kelemen, G. N. George, M. L. Gorbaty, *Fuel Processing Technology* **1990**, *24*, 425–429.
[22] G. P. Huffman, S. Mitra, F. E. Huggins, N. Shah, S. Vaidya, F. Lu, *Energy Fuels* **1991**, *5*, 574–581.
[23] G. S. Waldo, R. M. K. Carlson, J. M. Moldowan, K. E. Peters, J. E. Penner-Hahn, *Geochimica et Cosmochimica Acta* **1991**, *55*, 801–814.
[24] D. Li, G. M. Bancroft, M. Kasrai, M. E. Fleet, X. Feng, K. Tan, *The Canadian Mineralogist* **1995**, *33*, 949–960.
[25] M. Kasrai, J. R. Brown, G. M. Bancroft, Z. Yin, K. H. Tan, *International Journal of Coal Geology* **1996**, *32*, 107–135.
[26] G. Sarret, J. Connan, M. Kasrai, G. M. Bancroft, A. Charrié-Duhaut, S. Lemoine, P. Adam, P. Albrecht, L. Eybert-Bérard, *Geochimica et Cosmochimica Acta* **1999**, *63*, 3767–3779.
[27] M. E. Fleet, *The Canadian Mineralogist* **2005**, *43*, 1811–1838.
[28] R. Wiltfong, S. Mitra-Kirtley, O. Mullins, B. Andrews, G. Fujisawa, J. Larsen, **2005**, DOI 10.1021/EF049753N.
[29] L. Zhang, C. Wang, Y. Zhao, G. Yang, M. Su, C. Yang, *Journal of Fuel Chemistry and Technology* **2013**, *41*, 1328–1335.
[30] S. Mitra-Kirtley, O. C. Mullins, A. E. Pomerantz, in *Applying Nanotechnology to the Desulfurization Process in Petroleum Engineering* (Ed.: T.A. Saleh), IGI Global, **2016**, pp. 53–83.
[31] J. Moon, P. D. Kalb, L. Milian, P. A. Northrup, *Cement and Concrete Composites* **2016**, *67*, 20–29.
[32] E. Y. Yu, I. J. Pickering, G. N. George, R. C. Prince, *Biochim. Biophys. Acta - Gen. Subj.* **2001**, *1527*, 156–160.
[33] Y. Dauphin, J.-P. Cuif, J. Doucet, M. Salomé, J. Susini, C. Terry Willams, *Journal of Structural Biology* **2003**, *142*, 272–280.
[34] J.-P. Cuif, Y. Dauphin, J. Doucet, M. Salome, J. Susini, *Geochimica et Cosmochimica Acta* **2003**, *67*, 75–83.
[35] E. Y. Sneeden, H. H. Harris, I. J. Pickering, R. C. Prince, S. Johnson, X. Li, E. Block, G. N. George, *J. Am. Chem. Soc.* **2004**, *126*, 458–459.

[36] I. J. Pickering, E. Y. Sneeden, R. C. Prince, E. Block, H. H. Harris, G. Hirsch, G. N. George, *Biochemistry* **2009**, *48*, 6846–6853.
[37] G. Veronesi, E. Koudouna, M. Cotte, F. L. Martin, A. J. Quantock, *Anal Bioanal Chem* **2013**, *405*, 6613–6620.
[38] Y. Tamenori, T. Yoshimura, N. T. Luan, H. Hasegawa, A. Suzuki, H. Kawahata, N. Iwasaki, *Journal of Structural Biology* **2014**, *186*, 214–223.
[39] J. Czapla-Masztafiak, K. Okoń, M. Gałka, T. Huthwelker, W. M. Kwiatek, *Appl. Spectrosc., AS* **2016**, *70*, 264–271.
[40] M. J. Hackett, G. N. George, I. J. Pickering, B. F. Eames, *Biochemistry* **2016**, *55*, 2441–2451.
[41] J. Perrin, C. Rivard, D. Vielzeuf, D. Laporte, C. Fonquernie, A. Ricolleau, M. Cotte, N. Floquet, *Geochimica et Cosmochimica Acta* **2017**, *197*, 226–244.
[42] A. Schmalenberger, W. Pritzkow, J. J. Ojeda, M. Noll, **2011**.
[43] M. Sandström, F. Jalilehvand, E. Damian, Y. Fors, U. Gelius, M. Jones, M. Salomé, *Proceedings of the National Academy of Sciences* **2005**, *102*, 14165–14170.
[44] P. Frank, F. Caruso, E. Caponetti, *Anal Chem* **2012**, *84*, 4419–4428.
[45] D. Solomon, J. Lehmann, C. Martínez, *Soil Science Society of America Journal - SSSAJ* **2003**, *67*, DOI 10.2136/sssaj2003.1721.
[46] G. Kar, J. Schoenau, A. Gillespie, G. Singh, D. Peak, *Soil Science Society of America Journal* **2019**, *83*, DOI 10.2136/sssaj2019.01.0008.
[47] A. Vairavamurthy, W. Zhou, T. Eglinton, B. Manowitz, *Geochimica et Cosmochimica Acta* **1994**, *58*, 4681–4687.
[48] M. J. Morra, S. E. Fendorf, P. D. Brown, *Geochimica et Cosmochimica Acta* **1997**, *61*, 683–688.
[49] Y. Takahashi, Y. Kanai, H. Kamioka, A. Ohta, H. Maruyama, Z. Song, H. Shimizu, *Environ. Sci. Technol.* **2006**, *40*, 5052–5057.
[50] S. D. Kelly, D. Hesterberg, B. Ravel, in *Methods of Soil Analysis Part 5—Mineralogical Methods*, John Wiley & Sons, Ltd, **2008**, pp. 387–463.
[51] A. Manceau, K. L. Nagy, *Geochimica et Cosmochimica Acta* **2012**, *99*, 206–223.
[52] F. Riquelme, P. Northrup, J. L. Ruvalcaba-Sil, V. Stojanoff, D. Peter Siddons, J. Alvarado-Ortega, *Appl. Phys. A* **2014**, *116*, 97–109.
[53] K. Takemoto, D. Bamba, M. Ogawa, T. Ohta, *Journal of Water and Environment Technology* **2016**, *14*, 82–89.
[54] C. V. Rose, S. M. Webb, M. Newville, A. Lanzirotti, J. A. Richardson, N. J. Tosca, J. G. Catalano, A. S. Bradley, D. A. Fike, *Geology* **2019**, *47*, 833–837.
[55] I. Winter, J. Hormes, M. Hiller, *Nuclear Instruments and Methods in Physics Research Section B: Beam Interactions with Materials and Atoms* **1995**, *97*, 287–291.
[56] K. Isegawa, D. Kim, H. Kondoh, *RSC Advances* **2018**, *8*, 38204–38209.
[57] H. Uemachi, Y. Tamenori, T. Itono, T. Masuda, T. Shimoda, A. Fujiwara, *Electrochimica Acta* **2018**, *281*, 99–108.
[58] H. Modrow, G. Calderon, W. H. Daly, G. G. B. de Souza, R. C. Tittsworth, N. Moelders, P. J. Schilling, *Journal of Synchrotron Radiation* **1999**, *6*, 588–590.
[59] U. Aygül, D. Batchelor, U. Dettinger, S. Yilmaz, S. Allard, U. Scherf, H. Peisert, T. Chassé, *J. Phys. Chem. C* **2012**, *116*, 4870–4874.
[60] H. Ikeura-Sekiguchi, T. Sekiguchi, *Jpn. J. Appl. Phys.* **2014**, *53*, 02BB07.
[61] J. Mårdalen, C. Riekel, H. Müller, *J Appl Cryst* **1994**, *27*, 192–195.
[62] M. Coric, N. Saxena, M. Pflüger, P. Müller-Buschbaum, M. Krumrey, E. M. Herzig, *J. Phys. Chem. Lett.* **2018**, *9*, 3081–3086.
[63] R. Rahmawati, S. Masuda, C.-H. Cheng, C. Nagano, S. Nozaki, K. Kamitani, K. Kojio, A. Takahara, N. Shinohara, K. Mita, K. Uchida, S. Yamasaki, *Macromolecules* **2019**, *52*, 6825–6833.

[64] G. Freychet, E. Gann, L. Thomsen, X. Jiao, C. R. McNeill, *J. Am. Chem. Soc.* **2021**, *143*, 1409–1415.
[65] G. Freychet, V. Lemaur, M. Jevric, D. Vu, Y. Olivier, M. Zhernenkov, M. R. Andersson, C. R. McNeill, *Macromolecules* **2022**, *55*, 4733–4741.
[66] D. Li, G. M. Bancroft, M. Kasrai, M. E. Fleet, B. X. Yang, X. H. Feng, K. Tan, M. Peng, *Phys Chem Minerals* **1994**, *20*, 489–499.
[67] A. Vairavamurthy, *Spectrochimica Acta Part A: Molecular and Biomolecular Spectroscopy* **1998**, *54*, 2009–2017.
[68] I. J. Pickering, R. C. Prince, T. Divers, G. N. George, *FEBS Letters* **1998**, *441*, 11–14.
[69] P. Frank, S. D. George, E. Anxolabéhère-Mallart, B. Hedman, K. O. Hodgson, *Inorg. Chem.* **2006**, *45*, 9864–9876.
[70] K. Rose, S. E. Shadle, M. K. Eidsness, Kurtz Donald M., R. A. Scott, B. Hedman, K. O. Hodgson, E. I. Solomon, *J. Am. Chem. Soc.* **1998**, *120*, 10743–10747.
[71] T. Glaser, B. Hedman, K. O. Hodgson, E. I. Solomon, *Acc. Chem. Res.* **2000**, *33*, 859–868.
[72] K. Ito, A. T. Ta, D. B. Bishop, A. J. Nelson, J. G. Reynolds, J. C. Andrews, *Microchemical Journal* **2005**, *81*, 3–11.
[73] R. Sarangi, S. DeBeer George, D. J. Rudd, R. K. Szilagyi, X. Ribas, C. Rovira, M. Almeida, K. O. Hodgson, B. Hedman, E. I. Solomon, *J. Am. Chem. Soc.* **2007**, *129*, 2316–2326.
[74] K. Peariso, M. E. Helton, E. N. Duesler, S. E. Shadle, M. L. Kirk, *Inorg. Chem.* **2007**, *46*, 1259–1267.
[75] B. E. Van Kuiken, M. R. Ross, M. L. Strader, A. A. Cordones, H. Cho, J. H. Lee, R. W. Schoenlein, M. Khalil, *Structural Dynamics* **2017**, *4*, 044021.
[76] M. Ochmann, A. Hussain, I. von Ahnen, A. A. Cordones, K. Hong, J. H. Lee, R. Ma, K. Adamczyk, T. K. Kim, R. W. Schoenlein, O. Vendrell, N. Huse, *J. Am. Chem. Soc.* **2018**, *140*, 6554–6561.
[77] H. Modrow, J. Hormes, F. Visel, R. Zimmer, *Rubber Chemistry and Technology* **2001**, *74*, 281–294.
[78] Y. Yasuda, A. Tohsan, W. Limphirat, Y. Ikeda, *Kobunshi Ronbunshu* **2015**, *72*, 16–21.
[79] K. Shirode, H. Kawai, H. Oe, N. Nakamura, S. Yagi, *e-Journal of Surface Science and Nanotechnology* **2020**, *18*, 262–267.
[80] R. Chauvistré, J. Hormes, E. Hartmann, N. Etzenbach, R. Hosch, J. Hahn, *Chemical Physics* **1997**, *223*, 293–302.
[81] A. Mijovilovich, L. G. M. Pettersson, F. M. F. de Groot, B. M. Weckhuysen, *J. Phys. Chem. A* **2010**, *114*, 9523–9528.
[82] M. Qureshi, S. H. Nowak, L. I. Vogt, J. J. H. Cotelesage, N. V. Dolgova, S. Sharifi, T. Kroll, D. Nordlund, R. Alonso-Mori, T.-C. Weng, I. J. Pickering, G. N. George, D. Sokaras, *Phys. Chem. Chem. Phys.* **2021**, *23*, 4500–4508.
[83] A. Rompel, R. M. Cinco, M. J. Latimer, A. E. McDermott, R. D. Guiles, A. Quintanilha, R. M. Krauss, K. Sauer, V. K. Yachandra, M. P. Klein, *PNAS* **1998**, *95*, 6122–6127.
[84] G. Almkvist, K. Boye, I. Persson, *J Synchrotron Rad* **2010**, *17*, 683–688.
[85] L. Davenport Huyer, B. Zhang, A. Korolj, M. Montgomery, S. Drecun, G. Conant, Y. Zhao, L. Reis, M. Radisic, *ACS Biomater. Sci. Eng.* **2016**, *2*, 780–788.
[86] H. Sekiyama, N. Kosugi, H. Kuroda, T. Ohta, *BCSJ* **1986**, *59*, 575–579.
[87] E. Damian Risberg, L. Eriksson, J. Mink, L. G. M. Pettersson, M. Yu. Skripkin, M. Sandström, *Inorg. Chem.* **2007**, *46*, 8332–8348.
[88] T. Araki, K. Seki, S. Narioka, Y. Takata, T. Yokoyama, T. Ohta, S. Watanabe, T. Tani, *Jpn. J. Appl. Phys.* **1993**, *32*, 434.

[89] B. Flemmig, H. Modrow, K. Heinz Hallmeier, J. Hormes, J. Reinhold, R. Szargan, *Chemical Physics* **2001**, *270*, 405–413.
[90] J. J. H. Cotelesage, M. J. Pushie, L. Vogt, M. Barney, A. Nissan, I. J. Pickering, G. N. George, *J. Phys. Chem. A* **2016**, *120*, 6929–6933.
[91] L. I. Vogt, J. J. H. Cotelesage, N. V. Dolgova, C. J. Titus, S. Sharifi, S. J. George, I. J. Pickering, G. N. George, *RSC Advances* **2020**, *10*, 26229–26238.
[92] L. J. Bellamy, in *The Infrared Spectra of Complex Molecules: Volume Two Advances in Infrared Group Frequencies* (Ed.: L.J. Bellamy), Springer Netherlands, Dordrecht, **1980**, pp. 195–220.
[93] D. G. Castner, K. Hinds, D. W. Grainger, *Langmuir* **1996**, *12*, 5083–5086.
[94] S.-Y. Ding, M. Dong, Y.-W. Wang, Y.-T. Chen, H.-Z. Wang, C.-Y. Su, W. Wang, *J. Am. Chem. Soc.* **2016**, *138*, 3031–3037.
[95] E. Block, A. A. Bazzi, L. K. Revelle, *J. Am. Chem. Soc.* **1980**, *102*, 2490–2491.
[96] M. Lemarié, T.-N. Pham, P. Metzner, *Tetrahedron Letters* **1991**, *32*, 7411–7414.
[97] Z. Wang, B. Mi, *Environ. Sci. Technol.* **2017**, *51*, 8229–8244.
[98] W. Cao, F. Dai, R. Hu, B. Z. Tang, *J. Am. Chem. Soc.* **2020**, *142*, 978–986.
[99] Y. Chen, F. Zi, X. Hu, P. Yang, Y. Ma, H. Cheng, Q. Wang, X. Qin, Y. Liu, S. Chen, C. Wang, *Separation and Purification Technology* **2020**, *230*, 115834.
[100] Z. Chen, D. Wang, S. Feng, H. Liu, *ACS Appl. Mater. Interfaces* **2021**, *13*, 23592–23605.
[101] M. Ahmad, T. Shah, M. R. Tariq, L. Zhang, Y. Lyu, W. Iqbal, M. ud-din Naik, A. Khosla, Q. Zhang, B. Zhang, *Journal of Cleaner Production* **2023**, *426*, 139012.
[102] G. Kaindl, G. Kalkowski, W. D. Brewer, B. Perscheid, F. Holtzberg, *Journal of Applied Physics* **1984**, *55*, 1910–1915.
[103] D. J. Smythe, J. M. Brenan, N. R. Bennett, T. Regier, G. S. Henderson, *Journal of Non-Crystalline Solids* **2013**, *378*, 258–264.
[104] M. A. Prusinkiewicz, F. Farazkhorasani, J. J. Dynes, J. Wang, K. M. Gough, S. G. W. Kaminskyj, *Analyst* **2012**, *137*, 4934–4942.
[105] P. Zhang, T. K. Sham, *Phys. Rev. Lett.* **2003**, *90*, 245502.
[106] D. Stellwagen, A. Weber, G. L. Bovenkamp, R. Jin, J. H. Bitter, C. S. S. R. Kumar, *RSC Adv.* **2012**, *2*, 2276–2283.
[107] W. Kurashige, S. Yamazoe, K. Kanehira, T. Tsukuda, Y. Negishi, *J. Phys. Chem. Lett.* **2013**, *4*, 3181–3185.
[108] D. M. Chevrier, X. Meng, Q. Tang, D. Jiang, M. Zhu, A. Chatt, P. Zhang, *J. Phys. Chem. C* **2014**, *118*, 21730–21737.
[109] A. L. Trigub, B. R. Tagirov, K. O. Kvashnina, D. A. Chareev, M. S. Nickolsky, A. A. Shiryaev, N. N. Baranova, E. V. Kovalchuk, A. V. Mokhov, *American Mineralogist* **2017**, *102*, 1057–1065.
[110] C. F. I. Shaw, M. P. Cancro, P. L. Witkiewicz, J. E. Eldridge, *Inorg. Chem.* **1980**, *19*, 3198–3201.
[111] G. Annibale, L. Canovese, L. Cattalini, G. Natile, *J. Chem. Soc., Dalton Trans.* **1980**, 1017–1021.
[112] A. G. Tathe, N. T. Patil, *Org. Lett.* **2022**, *24*, 4459–4463.
[113] L. T. Ball, G. C. Lloyd-Jones, C. A. Russell, *J. Am. Chem. Soc.* **2014**, *136*, 254–264.
[114] P. Römbke, A. Schier, H. Schmidbaur, *J. Chem. Soc., Dalton Trans.* **2001**, 2482–2486.
[115] A. Nardelli, G. Fronzoni, M. Stener, *J. Phys. Chem. C* **2009**, *113*, 14844–14851.
[116] J. A. Bearden, A. F. Burr, *Rev. Mod. Phys.* **1967**, *39*, 125–142.
[117] A. Owens, S. C. Bayliss, P. J. Durham, S. J. Gurman, G. W. Fraser, *The Astrophysical Journal* **1996**, *468*, 451.
[118] M. K. Kiesewetter, E. J. Shin, J. L. Hedrick, R. M. Waymouth, *Macromolecules* **2010**, *43*, 2093–2107.

[119] A. P. Dove, *ACS Macro Lett.* **2012**, *1*, 1409–1412.
[120] J. U. Pothupitiya, N. U. Dharmaratne, T. M. M. Jouaneh, K. V. Fastnacht, D. N. Coderre, M. K. Kiesewetter, *Macromolecules* **2017**, *50*, 8948–8954.
[121] R. Frahm, *Nuclear Instruments and Methods in Physics Research Section A: Accelerators, Spectrometers, Detectors and Associated Equipment* **1988**, *270*, 578–581.
[122] A. H. Clark, P. Steiger, B. Bornmann, S. Hitz, R. Frahm, D. Ferri, M. Nachtegaal, *J Synchrotron Rad* **2020**, *27*, 681–688.
[123] A. J. Dent, G. Cibin, S. Ramos, S. A. Parry, D. Gianolio, A. D. Smith, S. M. Scott, L. Varandas, S. Patel, M. R. Pearson, L. Hudson, N. A. Krumpa, A. S. Marsch, P. E. Robbins, *J. Phys.: Conf. Ser.* **2013**, *430*, 012023.

X-ray absorption spectroscopy is used to determine sulfur speciation following an oxidative crosslinking treatment that transforms polythionolactones into degradable, elastic polymers, revealing the presence of thionoesters, disulfides, thioethers, sufones, and – surprisingly – sulfate esters. Quantitative linear combination analysis reveals that speciation is strongly dependent on the size of the monomer aliphatic chain in each polymer and ultimately impacts physical properties such as porosity and density. The nature of gold binding by these polymers is also explored.

Melissa A. Smith, U. L. D. Inush Kalana, George E. Sterbinsky, Tianpin Wu, Matthew K. Kiesewetter,* and Dugan Hayes*

**Determining sulfur speciation in oxidatively crosslinked degradable polymers using sulfur K-edge X-ray absorption spectroscopy**